Journal of Experimental Botany, Vol. 72, No. 12 pp. 4489–4501, 2021
doi:10.1093/jxb/erab100 Advance Access Publication 19 March 2021

RESEARCH PAPER

Aquaporins, and not changes in root structure, provide new insights into physiological responses to drought, flooding, and salinity

Jean-Christophe Domec[1,2,*], John S. King[3], Mary J. Carmichael[4], Anna Treado Overby[5], Remi Wortemann[6], William K. Smith[7], Guofang Miao[8], Asko Noormets[9] and Daniel M. Johnson[10]

[1] Bordeaux Sciences AGRO, UMR1391 ISPA INRA, 1 Cours du général de Gaulle, 33175 Gradignan Cedex, France
[2] Nicholas School of the Environment, Duke University, Durham, NC 27708, USA
[3] Department of Forestry and Environmental Resources, North Carolina State University, Raleigh, NC 27606, USA
[4] Departments of Biology and Environmental Studies, Hollins University, Roanoke, VA 24020, USA
[5] Planning, Design and the Built Environment, Clemson University, Clemson, SC 29634, USA
[6] Université de Lorraine, INRA, UMR 1434 Silva, 54000, Nancy, France
[7] Department of Biology, Wake Forest University, Winston-Salem, NC 27109, USA
[8] School of Geographical Sciences, Fujian Normal University, Fuzhou, FJ-350007, PR China
[9] Department of Ecology and Conservation Biology, Texas A&M University, College Station, TX 77843, USA
[10] Warnell School of Forestry and Natural Resources, University of Georgia, Athens, GA 30602, USA

* Correspondence: jc.domec@duke.edu

Received 27 October 2020; Editorial decision 23 February 2021; Accepted 27 February 2021

Editor: Jianhua Zhang, Hong Kong Baptist University, Hong Kong

Abstract

The influence of aquaporin (AQP) activity on plant water movement remains unclear, especially in plants subject to unfavorable conditions. We applied a multitiered approach at a range of plant scales to (i) characterize the resistances controlling water transport under drought, flooding, and flooding plus salinity conditions; (ii) quantify the respective effects of AQP activity and xylem structure on root (K_{root}), stem (K_{stem}), and leaf (K_{leaf}) conductances; and (iii) evaluate the impact of AQP-regulated transport capacity on gas exchange. We found that drought, flooding, and flooding plus salinity reduced K_{root} and root AQP activity in *Pinus taeda*, whereas K_{root} of the flood-tolerant *Taxodium distichum* did not decline under flooding. The extent of the AQP control of transport efficiency varied among organs and species, ranging from 35–55% in K_{root} to 10–30% in K_{stem} and K_{leaf}. In response to treatments, AQP-mediated inhibition of K_{root} rather than changes in xylem acclimation controlled the fluctuations in K_{root}. The reduction in stomatal conductance and its sensitivity to vapor pressure deficit were direct responses to decreased whole-plant conductance triggered by lower K_{root} and larger resistance belowground. Our results provide new mechanistic and functional insights on plant hydraulics that are essential to quantifying the influences of future stress on ecosystem function.

Keywords: Anatomy, aquaporin activity, bald cypress, conductances, flooding, leaf water relations, loblolly pine, *Pinus taeda*, plant hydraulics, *Taxodium distichum*, water stress.

Introduction

There is scientific consensus that the Earth's climate is changing at a geologically unprecedented rate and that human activities are a contributing factor, indicated by the National Academy of Sciences survey on climate change (NAS, 2020), and bolstered by a recent IPCC report (Oppenheimer *et al.*, 2019). Due to a combination of seawater thermal expansion and melting of glaciers and polar ice sheets, the global sea level rose 0.32 m over the 20th century and is projected to rise by an extra 0.82 m by 2100 (Woodruff *et al.*, 2013). Coastal forests are among the world's most biologically diverse and productive ecosystems, but unfortunately are also the most vulnerable to sea level rise (SLR; Kirwan and Gedan, 2019). In addition to increased flooding, SLR is globally expected to foster high salinities into tributary freshwater areas of the coastal zones (Bhattachan *et al.*, 2018). At the same time as being subject to increased salinity, those threatened ecosystems undergo periodic droughts, exposing coastal forests to low soil water availability (DeSantis *et al.*, 2007). Understanding forest responses to SLR therefore requires the determination of physiological response mechanisms to drought, flooding, and flooding plus salinity.

Scientists have a broad-scale understanding of plant adjustment and tolerance to flooding and salinity along environmental gradients, and the bulk of recent work in plants has been crucial in distinguishing adaptive plant strategies (Kirwan and Gedan, 2019). One of the most characteristic traits of wetland plants is aerenchyma, a specialized tissue made of intercellular gas-filled spaces that improves the storage and diffusion of oxygen. Overall, the physiological responses of plants to salt stress and flooding are similar in many ways (Allen *et al.*, 1996; Munns, 2002), but the mechanisms by which plants deal with these stressors differ across species (Munns and Tester, 2008). The main consensus is that the primary response of plants to flooding and salt is inhibition of root hydraulic conductance (Loustau *et al.*, 1995; Rodríguez-Gamir *et al.*, 2012). In turn, this reduction in water uptake capacity reduces photosynthesis and growth due to the closure of stomata (McLeod *et al.*, 1996; Munns and Tester, 2008). However, there are no studies that have focused on variation in hydraulic traits in contrasting species in terms of root physiological adaptive strategies to full inundation, limiting our understanding of how they are linked to leaf- and whole-plant-level water transport, which restricts our ability to predict forest ecophysiological response to SLR and climate change.

Water flow in the soil–plant–atmosphere continuum (SPAC) is determined by the hydraulic conductance of soil and plant tissues, which characterizes the structural capacity of the whole plant to move water (Tyree and Zimmermann, 2002). Hydraulic conductance (K_{plant}) is an important factor predicting gas exchange, transpiration, plant water status, growth rate, and resistance to environmental stresses (Brodribb and Holbrook, 2003; Sperry, 2003; Addington *et al.*, 2004; McCulloh *et al.*, 2019). The partitioning of K_{plant} along the water transport path is very variable, not only among species, but also diurnally and among plant organs (Ye and Steudle, 2006; Johnson *et al.*, 2016). Approximately 50–60% of the whole-plant hydraulic resistances ($1/K_{plant}$) are located in the root system, which shows the outstanding importance of this organ within the flow path (see review by Tyree and Zimmermann, 2002). Peripheral organs such as leaves and roots have been proposed as possible replaceable hydraulic fuses of the SPAC during stress, uncoupling stems hydraulically from transpiring surfaces and soil (Hacke *et al.*, 2000; Sperry, 2003; Domec *et al.*, 2009; Johnson *et al.*, 2016). Quantifying the relative contribution of K_{root} to K_{plant} and how it varies under drought, flooding, and flooding plus salinity is thus essential for understanding how these stressors influence photosynthesis and stomatal conductance (g_s) and their sensitivity to climatic variables. In addition, mechanistic depiction of variation in K_{plant} and its impact on g_s, and the sensitivity of g_s to prominent environmental drivers, requires isolating the main resistances to plant water flow, and their dynamics in response to abiotic stress factors, which has rarely been done.

Most research on abiotic stresses has focused on aboveground organs and neglected physiological responses of flow dynamics in roots, especially in woody plants. This is surprising because important processes of plant tolerance are located in the roots and also because roots are the first organs to be affected by water stress, flooding, and salinity (Krauss *et al.*, 1999). In radial and axial roots axes, resistance to water flow depends on root anatomy (Knipfer and Fricke, 2011), whereas in the radial component it is also a function of protein water channels, or aquaporins (AQPs), that regulate the resistance of the transcellular pathway (Chaumont *et al.*, 2005; Gambetta *et al.*, 2017). AQPs are imbedded in the plasma and vacuolar membranes of most root cell types, and form pores that are highly selective for water (Törnroth-Horsefield *et al.*, 2006). In crop plants, AQP chemical inhibitors (i.e. mercuric chloride or hydroxyl radicals) demonstrated that AQP down-regulation is the principal cause of alterations of the radial pathway, resulting in a decrease in K_{root} (Ehlert *et al.*, 2009; Knipfer and Fricke, 2011; Maurel and Nacry, 2020). Compared with reference plants used in molecular studies such as corn, tobacco, and Arabidopsis (Siefritz *et al.*, 2002; Boursiac *et al.*, 2008; Bramley *et al.*, 2009; Tan and Zwiazek, 2019), the significance of AQP regulation in woody plants and its effect within the SPAC is still poorly understood (Gambetta *et al.*, 2013; Johnson *et al.*, 2014; Rodriguez-Gamir *et al.*, 2019). In addition, little work has addressed the importance of species differences in root AQP functioning in response to environmental stresses.

Better information on physiological functioning of forest species in stressed environments is needed to develop adaptive management strategies that will help protect threatened coastal ecosystems (Carmichael and Smith, 2016). To fully understand the impacts of SLR on plant adaptation, the influence of abiotic stresses on root hydraulics must be evaluated with respect

to the entire capacity of the plant to move water. This is especially relevant for seedlings, which have low physiological capacity to tolerate many stressors (Niinemets, 2010), impacting species persistence under changing conditions (Megonigal and Day, 1992; Brodersen *et al.*, 2019). In that framework, our first objective was to characterize the vascular conductances that control water movement through the plant system under drought, flooding, and flooding plus salinity stresses. Our second objective was to quantify the effects of AQP activity on plant organs and partition the antagonistic effects of AQP and xylem structure on conductances. Our third objective was to evaluate a hypothesized correlation between leaf-level gas exchange and AQP regulation of water transport under varying environmental conditions. Using contrasting species, we tested the hypotheses that a decrease in hydraulic conductance between treatments (i) is controlled by AQP activity rather than by a change in root xylem structure, with greater declines in stress-intolerant plants, and in roots than in stems and leaves; and (ii) is optimized in plants experiencing lower AQP inhibition, such that K_{root} exerts greater control on K_{plant}, which in turn affects g_s and carbon assimilation when environmentally stressed.

Materials and methods

Plant material and greenhouse experiments

We used 50 one-year-old *Taxodium distichum* L. and *Pinus taeda* L. half-sib seedlings supplied by ArborGen Inc. (Ridgeville, SC, USA). At the beginning of the spring season (late March), the seedlings were potted in 19 liters of commercial plant pots filled with a Fafard-4P soil mixture composed of sphagnum peat moss (50%), bark (25%), vermiculite (15%), and perlite (Fafard Inc., Agawam, MA, USA). This mixture was representative of the soil texture and organic matter content of soils found in coastal forested wetlands. Potted plants were maintained in a greenhouse with a 16 h photoperiod where daytime mean temperature and relative humidity were kept at 23±3 °C and 55±6%, respectively. Before the treatments were applied, all 50 plants were watered three times a week. Eight weeks after the beginning of the experiment, 36 plants were randomly separated into four groups (control, droughted, flooded, and flooded plus salt) and were surrounded and buffered by the 14 plants that were not used for the measurements. These treatments were intended to represent stresses related to SLR and periodic droughts exposing coastal forests, and thus the soil salinity treatment with no flooding was not studied. Those single-factor experiments were conducted simultaneously and applied for 35 d (Rodriguez-Gamir *et al.*, 2019). Control plants were irrigated with 2 liters of water twice per week, which was enough to saturate the substrate. For the drought treatment, plants were never irrigated from the start until the end of the experiment (Rodriguez-Gamir *et al.*, 2019). Flooding and flooding plus salinity was imposed by submerging the seedlings to the root collar (3 cm above the surface) without draining the pots (Pezeshki, 1992). The salinity treatment (concentration of 4 g l^{-1}, or 4 ppt) was prepared using a commercial seawater mixture (24 g l^{-1} NaCl; 11 g l^{-1} $MgCl_2 \cdot 6H_2O$; 4 g l^{-1} Na_2SO_4; 2 g l^{-1} $CaCl_2 \cdot 6H_2O$; 0.7 g l^{-1} KCl).

Hydraulic conductance of root, shoot. and whole plant

Five weeks after the treatments were applied, root (K_{root}), shoot (K_{shoot}), and stem (K_{stem}) hydraulic conductance were directly measured using a Hydraulic Conductance Flow Meter (HCFM; Tyree *et al.*, 1993) (Dynamax Inc., Houston, TX, USA). Hydraulic parameters were determined in six loblolly pine and five bald cypress seedlings per treatment, and conductance values for a given plant were obtained from the same plant. To minimize the potential impact of diurnal periodicity on hydraulic conductance, all measurements were taken between 10.00 h and 12.00 h, and under the same environmental conditions (temperature of 22 °C and relative humidity of 60%). During HCFM measurements, the leaves were submerged in water to maintain constant temperature and prevent transpiration. To measure K_{root} and K_{shoot}, the plants were cut 5 cm above the soil surface and the cut ends of the shoots and roots were connected to the HCFM. This instrument perfuses degassed water through the root or shoot system by applying pressure to a water-filled bladder contained within the unit. K_{root} was determined between 2 min and 4 min after shoot decapitation, thus minimizing measurement errors to <10% (Vandeleur *et al.*, 2014; Rodriguez-Gamir *et al.*, 2019; see also Supplementary Fig. S1). The flow rate of water through the root or shoot was determined under transient mode (Yang and Tyree, 1994), which consists of measuring flow rate under increasing pressure applied by a nitrogen gas cylinder. Transients were also performed on shoots after removal of leaves to determine K_{stem}. The applied pressure gradually rose from 0 to 450 kPa over the course of ~1 min and the flow rate at each pressure value was logged every 2 s using the Dynamax software. Hydraulic conductance (K) was then calculated using the formula: $K = Q_v/P$; where Q_v is the volumetric flow rate (kg s^{-1}) and P is the applied pressure (MPa). Hydraulic conductance was standardized to values for 25 °C to account for the effects of temperature on water viscosity. Because the HCFM operates under high pressure, the measured K_{root} and K_{shoot} represent maximum values of conductances, that is in the absence of embolized conduits. At the end of the measurements, projected leaf area of needles present on the shoots was determined with an LI-3100 leaf area meter (Li-Cor, Inc., Lincoln, NE, USA), then converted to all-sided leaf area (Wang *et al.*, 2019), and conductance values were expressed on a leaf specific area basis (Yang and Tyree, 1994). All plant biomass fractions were then harvested, dried at 70 °C for 48 h, and weighed. Further, mass-specific root hydraulic conductance ($K_{root\_biomass}$) was calculated by normalizing K_{root} by root dry mass.

Root (two opposite lateral roots per seedling taken ~2.5 cm down from the root collar were sampled) and stem tracheids were visualized by perfusing the decapitated samples with 0.1% toluidine blue and imaged at ×90–180 magnification using a digital camera mounted on a widefield zoom stereo microscope (ZM-4TW3-FOR-9M AmScope, USA). Tracheid diameter was measured along four radial rows per sample using an image analysis software (Motic Images version 3.2, Motic Corporation, China). In addition, the presence or absence of aerenchyma was assessed on four lateral roots per sample, which included the two used for tracheid size determination (no aerenchyma was present in the stems).

Whole-plant hydraulic resistance was calculated as in Domec *et al.* (2016)

$$1/K_{plant} = 1/K_{root} + 1/K_{shoot} \quad (1)$$

and resistances of the shoot components ($1/K_{stem}$ and $1/K_{leaf}$) were calculated from the difference between resistances before and after removal of each leaf. Hydraulic conductance and resistance are reciprocals, and the latter is used for partitioning the resistances in the root-to-leaf continuum, and the former for examining the coordination between plant hydraulics and gas exchange.

Aquaporin contribution to hydraulic conductances

We quantified the AQP contribution to K_{root} and K_{shoot} (and its components) and K_{plant} using hydroxyl radicals (·OH) produced using the Fenton reaction (solution made by equal mixing of 0.6 mM H_2O_2 and 3 mM $FeSO_4$) to inhibit AQP activity (Ye and Steudle, 2006; McElrone

et al., 2007; Boursiac et al., 2008). Hydroxyl radicals have been shown to be less toxic and above all more effective in blocking water channels than mercuric chloride (Henzler and Steudle, 2004) or acid loading (fig. 2 in Ehlert et al., 2009) of the solution surrounding the roots. Conductances with AQP function inhibited were measured by introducing ~18 ml of ·OH solution, instead of water, into the existing compression couplings connected to the sample and the HCFM (McElrone et al., 2007; Johnson et al., 2014). As previously measured (Boursiac et al., 2008; Almeida-Rodriguez et al., 2011; Rodriguez-Gamir et al., 2019), the effect of ·OH on conductivity was effective and reversible in <6 min when radicals were replaced with distilled water (Supplementary Fig. S1). Six transient curves per sample were constructed with the HCFM: two before inhibiting AQP activity, two after AQP inhibition, and two final ones after flushing the samples with water only to reassess the flow rate with no AQP inhibition. We calculated the AQP contribution to K_{root}, K_{shoot} (K_{stem} and K_{leaf}), and K_{plant} as the difference between initial conductance and conductance after AQP inhibition, divided by the initial conductance (Rodriguez-Gamir et al., 2019).

From measurements of conductances before and after inhibiting AQP activity, we were able to calculate whether the departure in values from control was due to either the xylem-only (structural changes in xylem conduits) or the AQP-only part of the hydraulic pathway. For a given stress applied, the structural part of the hydraulic pathway reducing conductance was calculated by dividing the difference in conductance between control and treatment after inhibiting AQP activity by the difference in conductance between control and treatment without inhibiting AQP activity. The AQP effect was taken as 1 minus the structural effect.

Gas exchange and water potential

Net photosynthesis (A) and g_s were measured with a Li-Cor 6400 (Li-Cor, Inc.). For each leaf, the chamber was set to match prevailing environmental conditions assessed immediately prior to the measurement: atmospheric CO_2 concentration (390–410 ppm), relative humidity (46–59%), photosynthetically active radiation (PAR; 1600–1800 μmol m^{-2} s^{-1}), and leaf temperature (21–26 °C). All gas exchange results were expressed on an all-sided leaf area basis, and only fully expanded healthy appearing needles of the same age were picked for analysis. Maximum (light-saturated) photosynthetic capacity (A_{sat}) was measured on four green branchlet needles per seedling grown in the upper third of the plants. Immediately after the gas exchange measurements were performed, leaf water potential (Ψ_{leaf}) was measured using a pressure chamber (PMS Instrument Company, Albany, OR, USA). To assess maximum (least negative) Ψ_{leaf}, two branchlets per individual from each treatment were sampled at predawn (between 05.00 h and 06.00 h).

Net photosynthesis versus intercellular CO_2 concentrations (A–Ci) curves were measured at 25 °C leaf temperature, 60±10% relative humidity, and 1600 μmol m^{-2} s^{-1} PAR. The chamber CO_2 concentrations were set to ambient and sequentially lowered to 50 ppm and then to 1500 ppm. These data were used to estimate the maximum Rubisco carboxylation (V_{cmax25}), the maximum electron transport (J_{max25}), and the dark respiration (R_{d25}) rates according to Farquhar et al. (1980).

Field hydraulic and canopy conductance

Two contrasting sites were used to determine field values of K_{plant} and g_s under typical field conditions, and droughted and flooded conditions of large trees growing in intact forests. Soil salinity never occurred at the field sites to our knowledge. The first study site is a forested wetland located at the Alligator River National Wildlife Refuge, on the Albemarle–Pamlico Peninsula of North Carolina, USA (35°47′N, 75°54′W). This research site was established in November 2008, and includes a 35 m instrumented tower for eddy covariance flux measurements, a micrometeorological station, and 13 vegetation plots spread over a 4 km^2 area (Miao et al., 2013; Domec et al., 2015). The forest type is mixed hardwood swamp forest (>100 years old); the overstorey is predominantly composed of water tupelo (*Nyssa aquatica* L.) that represents 39% of the basal area, and an even mix of red maple (*Acer rubrum* L.), bald cypress, and loblolly pine. The canopy of this site is fairly uniform, with heights ranging from 16 m to 21 m, and with leaf area index peaking at 4.0±0.3 in early July.

The second, drier site (35°11′N, 76°11′W) is located within the lower coastal plain, mixed forest province of North Carolina (Domec et al., 2009). This 100 ha mid-rotation (23-year-old) loblolly pine stand (US-NC2 in the Ameriflux database) was established in 1992 and has an understorey comprised of other woody species such as sparse red maple and bald cypress trees. Artificial drainage lowers the height of the water table, improving site access and increading productivity, especially during winter months (Domec et al., 2015).

At both sites, canopy conductance was derived from sapflow measurements and thus comprises the total water vapor transfer conductance from the 'average' stomata of the canopy. Sapflow was measured at breast height using thermal dissipation probes inserted in two flood-adapted species (bald cypress and water tupelo) and two others not adapted to flooding (red maple and loblolly pine) (see Domec et al., 2015 for further description of the sites and the methodology used). Note that water tupelo was only present at the wetland site. Stomatal conductance of the plants measured in the field was calculated from transpiration and vapor pressure deficit (VPD), using the simplification of the inversion of the Penman–Monteith model (Ward et al., 2013). To analyze the effect of K_{plant} on g_s, K_{plant} from field and greenhouse samples was calculated from the slope of the relationship between diurnal variation in Ψ_{leaf} and transpiration (Loustau et al., 1995). Changes in Ψ_{leaf} from dawn to mid-afternoon were quantified with a pressure chamber (PMS) on 6–8 leaves collected from each tree equipped with sapflow sensors.

Oren et al. (1999) showed that under saturated light, the decrease in g_s with increasing VPD is proportional to g_s at low VPD. Therefore, the sensitivity of the stomatal response to VPD when PAR was >800 μmol m^{-2} s^{-1} (light-saturated g_s) was determined by fitting the data to the functional form:

$$g_s = b - a\ln(\mathrm{VPD}) \quad (2)$$

where b is g_s at VPD=1 kPa (hereafter designated as reference or maximum canopy-averaged stomatal conductance, g_{s_max}), and a is the rate of stomatal closure and reflects the sensitivity of g_s to VPD [$dg_s/d\ln$VPD, in mmol m^{-2} s^{-1} $\ln(kPa)^{-1}$]. We propose to use this framework where VPD and light intensity are fixed to investigate the nature of the relationship between K_{plant} and g_{s_max}, and how this relationship affects the sensitivity of g_s to VPD.

Statistical analyses

All measured parameters were tested using multiple ANOVA with species, treatments, and AQP activity taken as factors. Mean separation was performed using the Tukey's procedure at the 95% confidence level. Statistical analyses were run using SAS (Version 9.4, Cary, NC, USA) and curve fits using SigmaPlot (version 12.5, SPSS Inc., San Rafael, CA, USA).

Results

Plant biomass

All treatments significantly reduced loblolly pine (*Pinus taeda* L.) total biomass (P<0.01; Table 1), whereas for the flood-tolerant bald cypress (*Taxodium distichum* L.) only the drought and the flooded plus salinity treatments had a negative effect

on growth (P<0.037). This decrease in plant growth was mainly attributed to a reduction in root and stem biomass in bald cypress (P<0.032), and in leaf and stem biomass in loblolly pine (P<0.01). Despite this reduction in plant size, the fine root to leaf mass ratio of bald cypress was only affected in the flooding plus salinity treatment, whereas in loblolly pine it was stimulated by 25% and 55% in the flooding and the flooding plus salinity conditions, respectively. All stresses decreased leaf mass per area (LMA) in loblolly pine (P<0.02). In bald cypress, LMA was only negatively affected by the drought and by the flooded plus salinity treatments (P<0.01). Field measurements indicated that unlike loblolly pine and red maple (*Acer rubrum* L.), flooded bald cypress and water tupelo (*Nyssa aquatica* L.) grew as rapidly (P>0.65) as trees subjected to periodic or non-flooded conditions (Supplementary Fig. S2).

Effect of flooding and salinity on the partitioning of hydraulic conductance

All treatments decreased whole-plant hydraulic conductance (K_{plant}) in loblolly pine (P<0.05), whereas bald cypress was only affected by the drought and the flooding plus salinity treatment (Fig. 1). In both species, the strongest decreases in root (K_{root}) and shoot (K_{shoot}) hydraulic conductances were measured for plants subjected to flooding plus salinity. It should be noted that flooding alone did not affect any of the conductances in bald cypress. When loblolly pines were flooded, even K_{root} on a root mass basis ($K_{root\_biomass}$) dropped significantly (by 45%), whereas K_{root} or $K_{root\_biomass}$ of the flood-tolerant bald cypress did not (Table 2; Fig. 1).

Under control conditions, roots represented between 35% and 45% of whole-plant resistance ($1/K_{plant}$) and, under treatments, root resistance partitioning increased by 15–40% (P=0.038) across both species. The overall decline in K_{plant} following treatments was mainly driven by an increase in root and stem resistances in loblolly pine, and by root resistance only in bald cypress (Fig. 2). In loblolly pine, this increase in root and stem resistance partitioning was paralleled by a 40% reduction (P=0.023) in leaf resistance partitioning (from 18% under control to 32–56% in the other treatments). In bald cypress, the flooded plus salt treatment increased the predominance of root resistance by >40% (P<0.001), which was accompanied by a decrease in the contribution of leaf and stem to the overall whole-plant resistance (Fig. 2).

Aquaporin contribution to plant organ conductances and gas exchanges

The reduction in K_{root} and K_{plant} between control and the other treatments (Fig. 1) was mainly caused by a reduction in AQP activity rather than by a change in root anatomy (Table 1; Fig. 3). Even when K_{root} was calculated on a root biomass basis ($K_{root\_biomass}$), the inhibition of AQP activity led to similar values of $K_{root\_biomass}$ (AQP-inhibited $K_{root\_biomass}$ in Table 2)

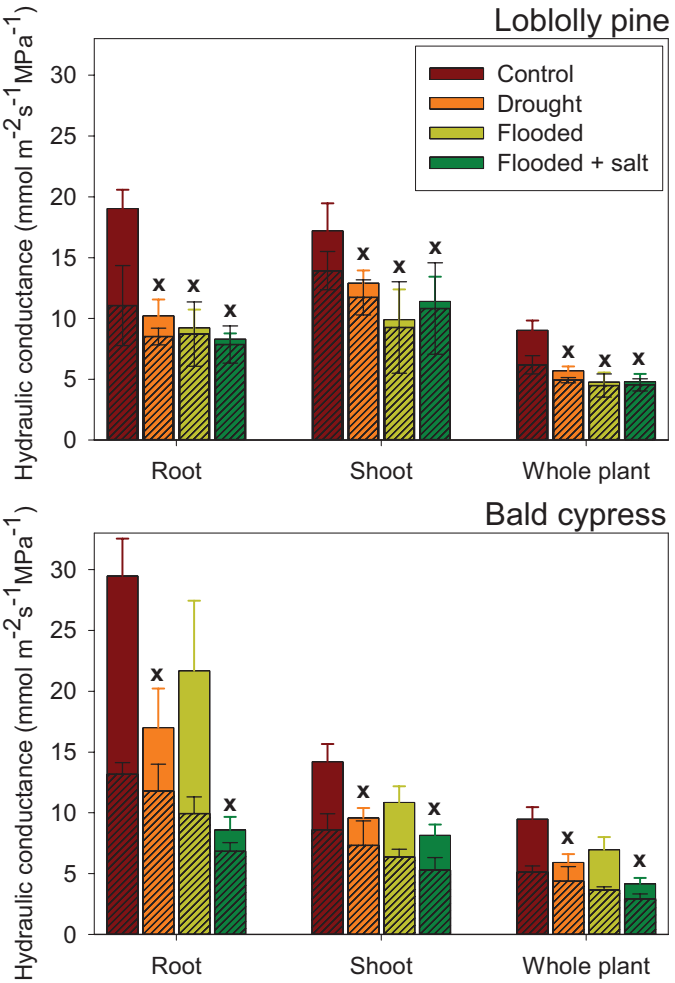

Fig. 1. Mean values (±SE) of hydraulic conductances (solid bars) in root, shoot, and whole loblolly pine (n=6) and bald cypress (n=5) plants growing in control, droughted, flooded, and flooded+salt conditions. Crosses indicate a significant difference between control and any of the treatments (P<0.05). Hashed bars represent values of hydraulic conductance following aquaporin inhibition, that is the xylem-only part of the hydraulic pathway.

across all treatments (P>0.47) in bald cypress, and for the flooded treatment (P=0.87) in loblolly pine. Nonetheless, in loblolly pine seedlings, AQP-inhibited $K_{root\_biomass}$ decreased by 31% (P=0.042) and 45% (P=0.028) in the drought and flooded plus salt treatments, respectively, but that was still less than the overall reduction in $K_{root\_biomass}$ (52% and 66%, respectively), indicating that changes in $K_{root\_biomass}$ were mostly driven by the inhibition of AQP. This reduction in $K_{root\_biomass}$ in loblolly pine mirrored the decrease in root and stem tracheid diameter in the drought and flooded plus salt treatments (Table 1). In bald cypress, tracheid size was not affected by treatment, but aerenchyma production was stimulated under flooded conditions (Table 1).

While blockage of AQP reduced hydraulic conductance, the extent of the decrease varied among organs and species. Root AQP activity in loblolly pine decreased (P<0.001) from

Table 1. Plant, root (fine plus coarse), stem, and leaf dry masses (g), as well as mean tracheid diameters (Dt_stem; Dt_root), fine root to leaf mass ratio ($Root_{fine}$/Leaf), and leaf mass per area (LMA) for the different treatments of *Taxodium distichum* (*n*=5, ±SE) and *Pinus taeda* (*n*=6, ±SE)

	Control		Drought		Flooded		Flooded plus salt	
	T. distichum	*P. taeda*	*T. distichum*	*P. taeda*	*T. distichum*	*P. taeda*	*T. distichum*	*P. taeda*
Plant (g)	13.9±1.1 c	10.7±0.4 b	9.9±0.9 ab	9.1±0.4 a	11.7±1.0 bc	9.5±0.6 a	9.7±0.8 ab	7.9±0.8 a
Root (g)	6.1±0.4 b	4.7±0.4 a	4.4±0.5 a	4.2±0.3 a	5.0±0.6 ab	4.9±0.4 a	3.9±0.5 a	4.3±0.3 a
Stem (g)	5.4±0.5 d	2.9±0.2 b	3.3±0.3 c	2.2±0.1 a	3.9±0.4 c	1.9±0.2 a	2.8±0.2 b	1.8±0.1 a
Leaf (g)	2.4±0.6 ab	3.1±0.4 b	2.2±0.4 b	2.6±0.3 b	2.8±0.8 ab	2.7±0.3b	2.9±0.7 ab	1.7±0.3 a
Dt_stem (μm)	23.1±3.8 c	14.8±2.1 b	19.9±2.2 c	9.4±1.2 a	22.6±4.1 c	13.6±1.5 ab	17.8±2.2 bc	10.2±1.5 a
Dt_root (μm)	12.3±0.9 c	10.2±1.0 bc	11.8±1.3 c	8.8±0.8 ab	13.3±1.6 c	9.0±0.6 b	10.7±1.1 bc	7.6±0.5 a
Aerenchyma	Yes – 38%	No	No	No	Yes – 84%	No	Yes – 24%	No
$Root_{fine}$/Leaf	0.72±0.09 b	0.53±0.05 a	0.74±0.10 b	0.50±0.06 a	0.71±0.12 ab	0.67±0.04 b	0.48±0.07 a	0.79±0.9 b
LMA (g cm^{-2})	9.1±0.9 b	13.4±0.7 d	7.0±0.6 a	11.8±0.5 c	8.9±1.0 b	11.4±0.8 c	7.2±0.4 a	9.0±0.6 b

The presence (Yes – and the percentage of roots affected) or absence (No) of root aerenchyma (intercellular air spaces) observed 5 weeks after initiating the treatments is also indicated.
Values in horizontal sequences not followed by the same letter are significantly different at the 0.05 level.

42% under controlled conditions to <5–17% in the different treatments, which was the driver of the decline in whole-plant AQP contribution (Fig. 4A). In this species, we found that flooding and flooding plus salinity reduced the AQP activity of the whole plants from 32% to <6% ($P<0.01$). In bald cypress, only the drought and flooded plus salt treatments reduced ($P<0.02$) AQP contribution to K_{root} or K_{plant} (Fig. 4B). For that species, the inhibition of AQP in the flooding treatment did not affect ($P=0.95$) K_{root} or K_{leaf}. In both species, drought also had a significant effect on AQP contribution to K_{leaf}, with a decrease from 17% to 9% ($P<0.03$) in loblolly pine, and from 44% to 23% ($P<0.001$) in bald cypress. In both species, there was no treatment effect on the contribution of AQP activity to K_{stem} ($P>0.42$).

Maximum stomatal conductance (g_{s_max}; i.e. g_s measured at a reference VPD of 1 kPa and under saturated light) for bald cypress was only negatively affected by drought and the flooding plus salt treatment (Table 2). In loblolly pines, g_{s_max} differed under flooded and flooded plus salt treatments, experiencing the smallest and the largest stomatal closure, respectively. The photosynthetic rate of both species was also negatively affected by treatments ($P<0.04$), with the strongest reduction for the drought and flooded plus salt treatments (Table 2). The disruption of photosynthesis concurred with a reduction in Rubisco carboxylating enzyme activities and the maximum electron transport rate (V_{cmax25} and J_{max25}, respectively; Table 2). Similarly, across species, dark respiration rates were only affected by the flooded plus salt treatments.

After taking into account the effect of VPD on g_s, K_{plant} had a major influence on g_{s_max} under field conditions. Across species and treatments, and whether plants were from the greenhouse or grown in the field, a 50% reduction in K_{plant} was accompanied by a 37% decline in g_{s_max} (Fig. 5A). There was indeed no difference ($P=0.33$) in the relationship between g_{s_max} and K_{plant} for seedlings growing in the greenhouse and mature trees in the field. Species differences were apparent in K_{plant}, with higher values in bald cypress and red maple. Flooded loblolly pine exhibited the same level of reduced K_{plant} as water-stressed plants. In red maple, permanently flooded conditions reduced water uptake capacity >2-fold, and this species exhibited higher hydraulic limitation and g_{s_max} in flooded than in drought-stressed conditions. However, bald cypress and water tupelo (circles and diamonds in Fig. 5A, respectively), which are species found in permanently wet soils, did not experience more than a 15% decline in g_{s_max} under flooded conditions. The sensitivity of g_s to VPD was linearly related to g_{s_max} (Fig. 5B) and K_{plant} (Supplementary Fig. S3A). Stomatal conductance declined in response to increasing VPD, and the magnitude of the reduction varied over the measurement period as shown by the decline in g_{s_max}. The slope of the relationship between g_{s_max} and the sensitivity of g_s to VPD (0.62±0.04) was not different ($P>0.99$; Fig. 5B) from the previously reported generic value of 0.60 based on a hydraulic model that assumes tight stomatal regulation of Ψ_{leaf} (Oren *et al.*, 1999). Maximum g_s and stomatal sensitivity to VPD decreased linearly with the increasing contribution of root hydraulic resistance ($1/K_{root}$) to $1/K_{plant}$ for both species (Supplementary Fig. S3B). Those negative relationships appeared also to be identical across treatments, with a 50% increase in resistance belowground resulting in a 56% reduction in g_{s_max} and in a 65% decrease in stomatal sensitivity to VPD.

The decreases in g_{s_max} and A_{sat} were linked to a decrease in AQP contribution to root conductance among treatments and also species ($P<0.039$; Fig. 6). Although weaker, those relationships still held when whole-plant AQP activity was compared with gas exchange, and a 25 % decrease in AQP contribution to K_{plant} was predicted to reduce g_{s_max} by 38% and A_{sat} by 30%.

Table 2. Mean root hydraulic conductance on a root mass basis ($K_{root\_biomass}$), root hydraulic conductance on a root mass basis after inhibiting aquaporin (AQP) activity (AQP-inhibited $K_{root\_biomass}$), leaf water potentials (Ψ_{leaf}), maximum stomatal conductance, light-saturated photosynthesis, and photosynthetic parameters at 25 °C (V_{cmax25}, J_{max25}, and R_{d25}) for the different treatments of *Taxodium distichum* and *Pinus taeda*

	Control		Drought		Flooded		Flooded plus Salt	
	T. distichum	*P. taeda*	*T. distichum*	*P. taeda*	*T. distichum*	*P. taeda*	*T. distichum*	*P. taeda*
$K_{root\_biomass}$ (g kg^{-1} s^{-1} MPa^{-1})	8.6±0.3 c	9.6±1.1 c	5.9±0.4 b	4.6±0.7 a	8.0 ±1.2 c	5.4±0.7 ab	5.0±1.4 ab	3.3±1.2 a
AQP-inhibited $K_{root\_biomass}$ (g kg^{-1} s^{-1} MPa^{-1})	3.9±0.3 a	5.6±0.7 b	4.0±0.1 a	3.8±0.7 a	3.4 ±0.4 a	5.1±0.6 b	3.7±0.5 a	3.1±0.7 a
Pre-dawn water potential (MPa)	–0.32±0.02 b	–0.24±0.01 a	–0.78±0.07 c	–0.93±0.08 c	–0.31±0.02 b	–0.39±0.05 b	–0.71±0.09 c	–0.77±0.09 c
Midday water potential (MPa)	–0.70±0.08 a	–1.18±0.07 b	–0.94±0.09 a	–1.29±0.07 b	–0.78±0.09 a	–1.22±0.11 b	–0.98±0.06 a	–1.38±0.10 b
Stomatal conductance (g_{s_max}, mmol m^{-2} s^{-1})	124±13 e	93±6 d	92±11 d	41±5 b	115±7 de	61±6 c	49±9 bc	25±3 a
Photosynthetic rate (A_{sat},µmol m^{-2} s^{-1})	7.0±0.5 c	6.1±0.4 c	4.2±0.5 b	4.3±0.6 b	6.2±0.7 c	4.4±0.8 b	3.3±0.5 b	1.8±0.2 a
Rubisco carboxylation capacity (V_{cmax25},µmol m^{-2} s^{-1})	44.9±6.2 d	33.2±5.2 cd	25.3±3.4 bc	21.7±2.5 b	34.9±3.8 cd	26.0±1.6 b	10.8±2.4 a	6.1±0.9 a
Maximum electron transport rate (J_{max25},µmol m^{-2} s^{-1})	66.3±5.6 d	52.3±4.1 c	39.1±3.2 b	32.5±3.3 b	55.7±6.1 cd	38.6±5.2 b	29.6±6.6 b	13.3±1.4 a
Dark respiration rate (R_{d25},µmol m^{-2} s^{-1})	0.22±0.04 bc	0.27±0.04 c	0.19±0.04 b	0.17±0.02 b	0.19±0.02 b	0.23±0.04 bc	0.12±0.02 a	0.10±0.01 a

Values are means ±SE (n=5–6). Values in horizontal sequences not followed by the same letter are significantly different at the 0.05 level.

Fig. 2. Partitioning of hydraulic resistances (1/conductance) of loblolly pine and bald cypress root, stem, and leaf in control conditions (left axis), and effect of treatments on the control of hydraulic resistance partitioning (right axis). Note that roots and leaves represented >70% of total whole-plant resistance.

Discussion

In US coastal regions from Maryland to Texas that are vulnerable to SLR (Titus and Richman, 2001; Kirwan and Gedan, 2019), many species such as bald cypress, water tupelo, red maple, and loblolly pine are ecologically dominant and commercially important. The first two species are fully adapted to partial or total soil flooding, and the other species are common to forest communities of estuarine woodlands (Pezeshki, 1992; Keeland and Sharitz, 1995). Bald cypress seedlings generally tolerate flooding, but marked with an initial reduction in growth (Allen *et al.*, 1996). However, within 3–5 years, seedlings generally recover from the stress imposed by developing pneumatophores (Megonigal and Day, 1992), explaining why flooded trees may grow as rapidly as trees subjected to non-flooded conditions (Supplementary Fig. S2). However, before this root formation occurs, the influence of AQP on control

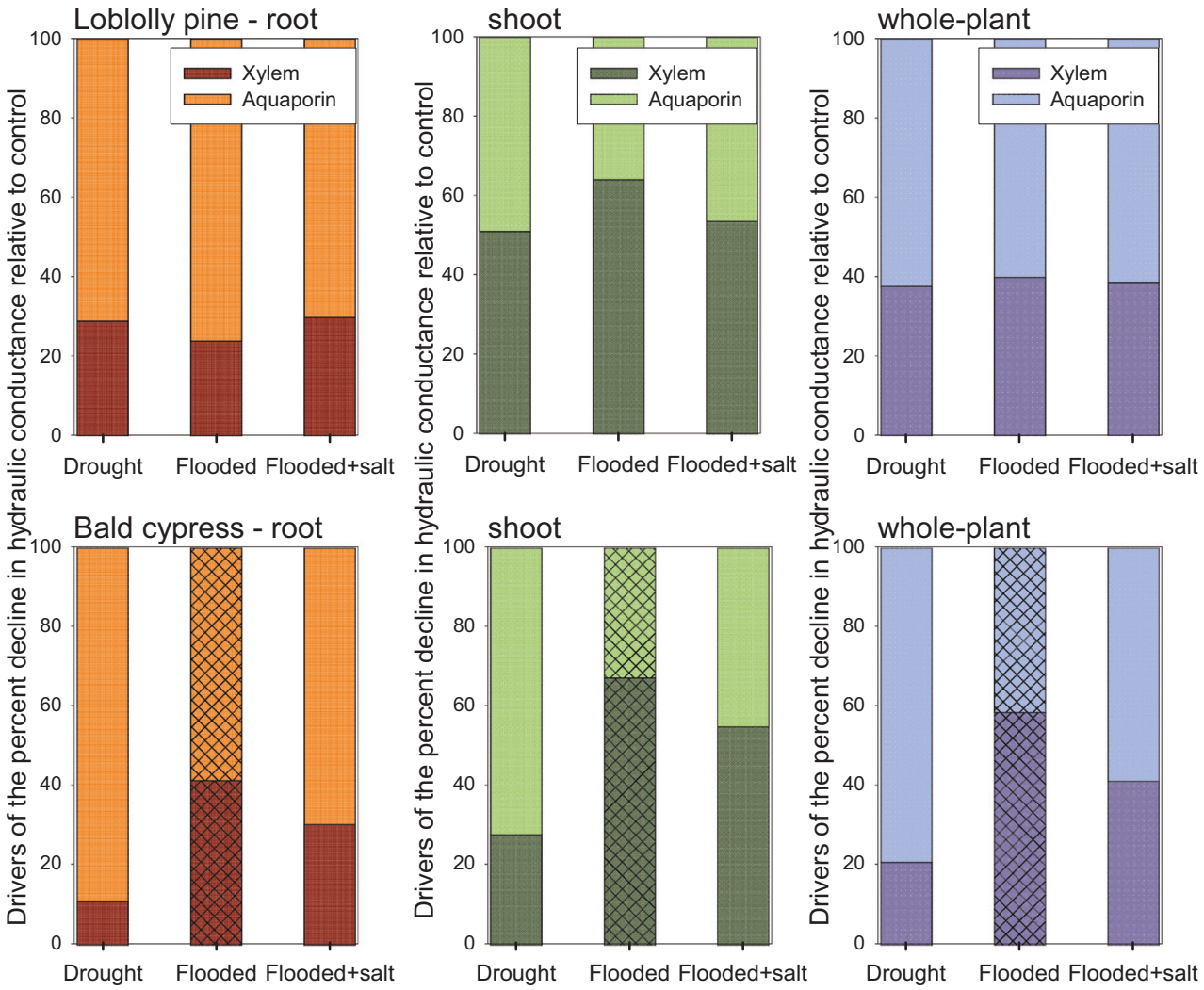

Fig. 3. Effect (shown as a percentage) of either the xylem-only (structural changes in xylem conduits) or the aquaporin-only (AQP) part of the hydraulic pathway on the decrease in loblolly pine and bald cypress hydraulic conductance between control and drought, flooded, and flooded plus salinity treatments (absolute values of conductances are seen in Fig. 1). For a given stress applied, the structural part of the hydraulic pathway reducing conductance was calculated by dividing the difference in conductance between control and treatment after inhibiting AQP activity by the difference in conductance between control and treatment without inhibiting AQP activity. The AQP effect was taken as 1 minus the structural effect. Bars with patterns represent treatments that did not induce significant difference in conductance (P>0.05; flooded condition for bald cypress).

of plant water movement and gas exchanges is needed, and is reflected in our results (Figs 4, 6).

Aquaporin activity appears to be essential in species-specific tolerance to stress

Our results highlight the integrated nature of hydraulics across the whole plant and emphasized the contributions of structural and physiological components to conductance (Bramley *et al.*, 2009; Maurel and Nacry, 2020). Drought, flooding, and flooding plus salinity treatments caused a significant shift in hydraulic resistance away from the stem and leaves to the roots, because of differential transmembrane AQP activity and not because of changes in the apoplastic hydraulic pathway (xylem diameter) (Table 1; Fig. 3; and see AQP-inhibited $K_{root\_biomass}$ in Table 2). During stress, some structural and anatomical changes also occurred, as seen by the decrease in either leaf, stem, or root biomass under drought or flooded plus salt treatments, affecting for the latter treatment root to leaf area ratio in both species (Table 1). However, and unlike the role played by AQP, those structural changes provided only minute adjustments in xylem hydraulic conductance (conductance once AQP activity was inhibited) and did not explain the whole decrease in conductance and thus the physiological mechanisms controlling water transport through the root (Table 2; Fig. 3). Both loblolly pine and bald cypress were highly susceptible to the combined stress of flooding plus salinity, which lends support to the role of saltwater intrusion in the formation of coastal ghost

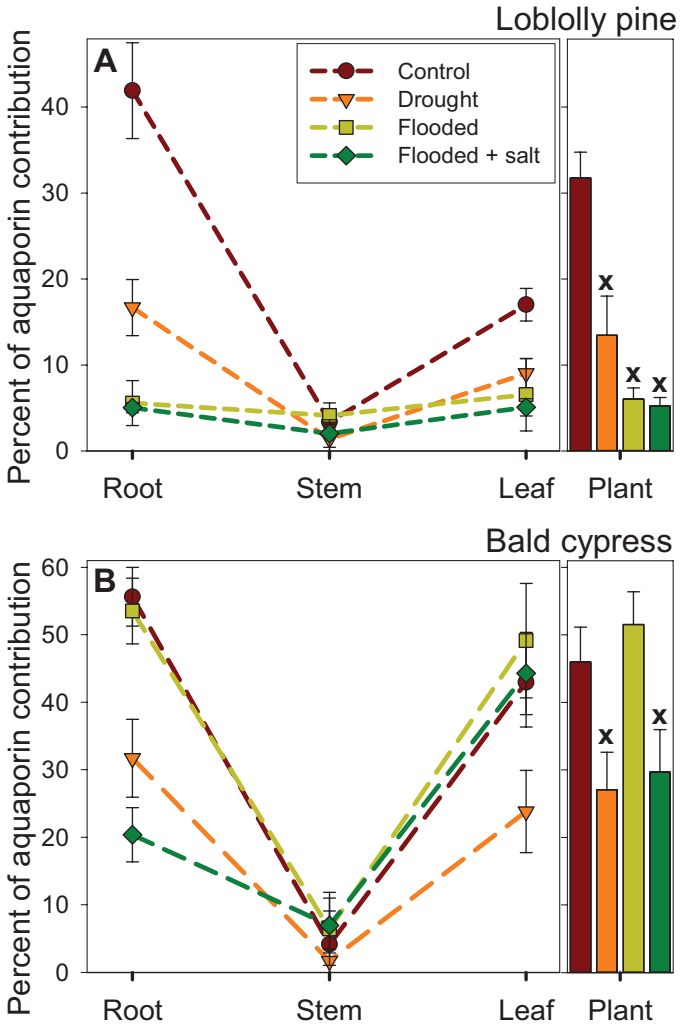

Fig. 4. Aquaporin (AQP) contribution to root, stem, leaf, and whole-plant hydraulic conductances in (A) loblolly pine (n=6, ±SE) and (B) bald cypress seedlings (n=5, ±SE) growing under control, water-stressed, flooded, and flooded plus salinity conditions. Crosses indicate a significant difference in whole-plant AQP contribution between control and any of the treatments (P<0.05).

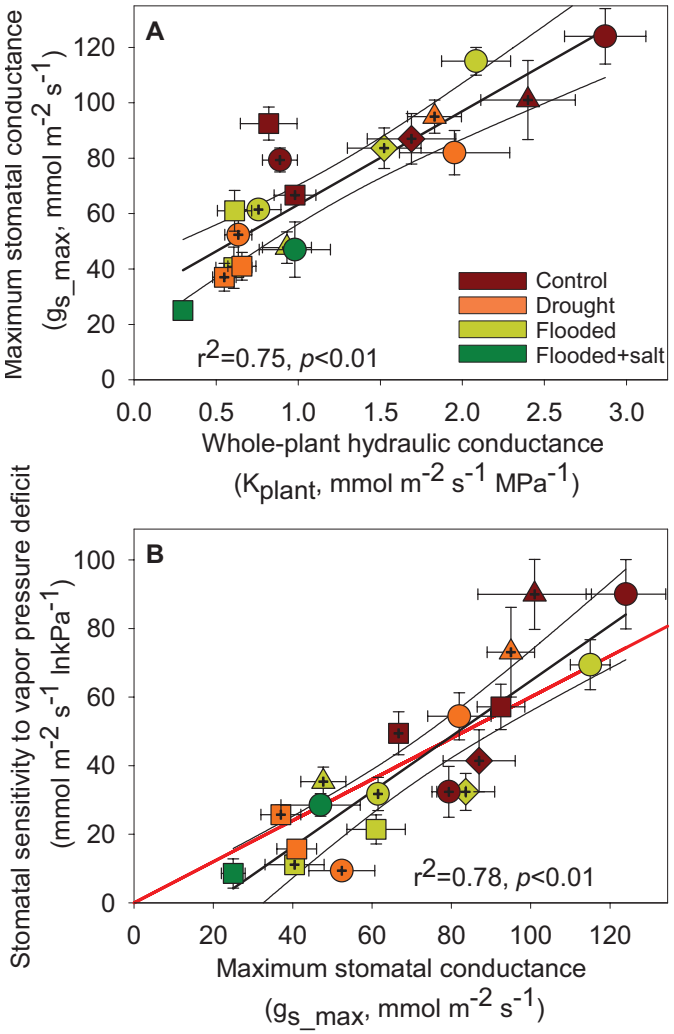

Fig. 5. (A) Linear relationship between the maximum (reference) stomatal conductance [g_s at vapor pressure deficit (VPD)=1 kPa] and (B) plant hydraulic conductance (K_{plant}) and between the sensitivity of stomatal conductance to VPD (dg_s/dlnVPD) and g_{s_max} of plant species growing under control, water-stressed, flooded, and flooded plus salinity conditions. Circles, diamonds, squares, and triangles represent bald cypress, water tupelo, loblolly pine, and red maple, respectively. Crossed-filled symbols represent mature plants growing in the field; non-crossed symbols represent bald cypress and loblolly pine seedlings from the greenhouse experiment. In (B), the red line (slope=0.6) indicates the theoretical slope between stomatal conductance at VPD=1 kPa and stomatal sensitivity to VPD that is consistent with the role of stomata in regulating minimum leaf water potential (Oren *et al.*, 1999).

forests, since bald cypress is also dying in these forests (Kirwan and Gedan, 2019). Lower pre-dawn Ψ_{leaf} values were expected with higher salinity because the lower osmotic potential of the medium (4 ppm corresponding to an osmotic potential of 0.31 MPa) probably increased leaf tissue ionic concentration (Allen *et al.*, 1996). This excess of ions disrupted photosynthesis and inhibited carboxylating enzyme activities (Table 2), which in turn contributed to inhibited root or leaf growth, and the production of new aerenchymatous roots in the flood-adapted species (Table 1).

These findings may shed light on the adaptive advantages of altering AQP activity in response to environmental stresses (Maurel and Nacry, 2020). Regarding drought, lowering AQP activity in roots should lead to larger Ψ_{leaf} gradients, inducing stomata to close more rapidly. Reducing water channel activity can then be seen as a means to reduce water loss when soil water availability is low (McLean *et al.*, 2011). In the case of flooding, the resulting decrease in K_{root} observed in the flood-intolerant species (such as loblolly pine used here) could also limit water transport to the leaves, causing stomatal closure and thus protecting the integrity of the whole hydraulic system until non-stressed conditions resume (Else *et al.*, 2001). Loblolly pine is known to be tolerant to low salinity and

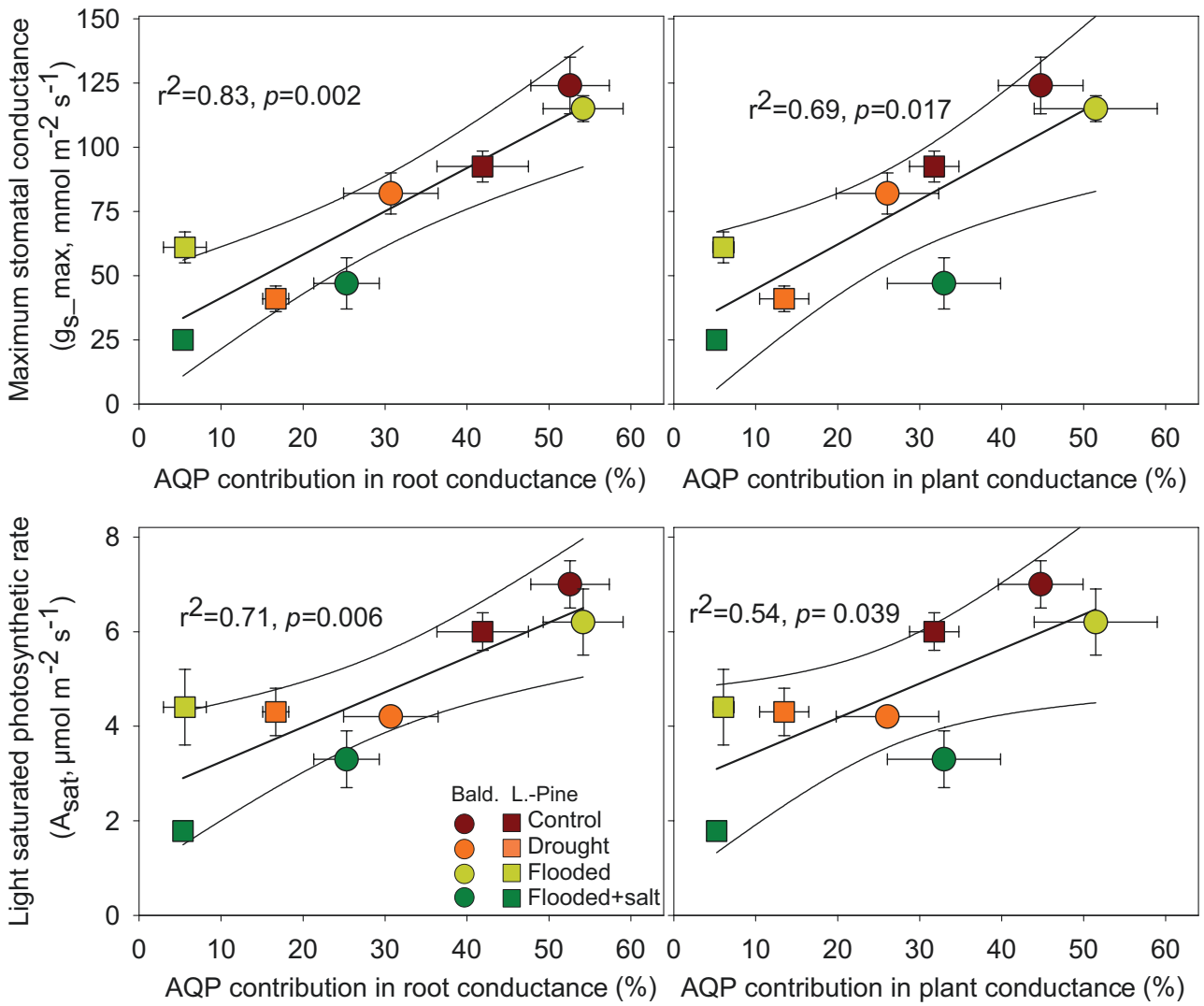

Fig. 6. Maximum stomatal conductance (g_{s_max}) and light-saturated photosynthetic rate (A_{sat}) versus aquaporin (AQP) contribution to root or whole-plant hydraulic conductances of bald cypress (Bald.) and loblolly pine (L.-Pine) seedlings growing under control, water-stressed, flooded, and flooded plus salinity conditions.

short-term flooding (Poulter *et al.*, 2008), and our experiment showed that this species significantly reduced gas exchange under these conditions, but to levels that were not lethal (Table 2). The negative impact of flooding on plants is a consequence of the low solubility of oxygen in water (Leyton and Rousseau, 1958), leading to anoxia (Kozlowski, 1997). The tight coupling of AQP functioning to the drop in cell energy (due to oxygen deprivation and acidosis) suggests that short-term adjustments in tissue hydraulics are critically needed during the early stages of the anoxic stress to balance water uptake with water loss (Tan *et al.*, 2019). Long-term metabolic adaptation to flooding is generally characterized by the decrease in belowground biomass to limit oxygen deficiency, but one of the most adaptive features of plants of wetland ecosystems is aerenchymatous tissues characterized by intercellular gas-filled spaces that improve the storage and diffusion of oxygen. Unlike the adjustment in root biomass or xylem anatomy that can take >2 months (Krauss *et al.*, 1999) and was not observed in any of the two seedlings (Table 1), intercellular air spaces, which were present after 5 weeks of flooding in bald cypress, probably played a vital role in maintaining root uptake and preventing the AQP-mediated reduction in K_{root}. Kamaluddin and Zwiazek (2002) and Holbrook and Zwieniecki (2003) have also proposed that anoxia-induced AQP down-regulation may prevent the transport of ethylene precursors away from the root, thereby favoring the accumulation of ethylene to trigger the differentiation of root aerenchymas, especially in adapted species such as bald cypress (Table 1). Salinity added to the flooding stress may trigger greater AQP inhibition, so that advective salt flow to the root surface may be minimized (Azaizeh and Steudle, 1991). In the short term (a few hours following exposure to flooding or flooding plus salinity), it has been shown that plants

respond to osmotic shock by reduced AQP activity (Martinez-Ballesta *et al.*, 2000; Rodríguez-Gamir *et al.*, 2012), which in our case was followed by reduced K_{root}, most probably as an adaptive strategy to eliminate water loss from the roots under conditions of low osmotic potential.

Finally, it can also be hypothesized that the role of AQP may in fact not concern the primary response of the plant to stress, but its recovery performance (Siefritz *et al.*, 2002). Stimulation of specific AQP suggested that 'gating' in response to salt stress involved not only the reduction in water channels, but also an enhancement in the internalization of specific AQPs (raft-associated pathway), putatively becoming active once stress is relieved (Li *et al.*, 2011).

Root hydraulics as related to whole-plant water transport and gas exchange

One of the objectives of our study was to evaluate a hypothesized correlation between leaf gas exchange and root hydraulics as influenced by AQP activity. The decline in g_{s_max} (and it is sensitivity to VPD) and photosynthesis was strongly related to the increase in root resistance due to a decrease in AQP contribution to K_{root}, with a common relationship found among the species despite important differences in treatment responses (Supplementary Fig. S3; Fig. 6). In non-woody plants, it has been suggested that abscisic acid (ABA) accumulation in leaves may be responsible for stomatal closure in flooded plants (Castonguay *et al.*, 1993; Else *et al.*, 2001). However, in woody plants, the marked reduction in g_s in flooded seedlings does not seem to be induced by ABA, since a significant reduction in g_s appeared a week after stressors were applied (Rodríguez-Gamir *et al.*, 2012), whereas the increase in ABA in leaves is generally detected 4–5 weeks later (Zhang and Zhang, 1994; Rodríguez-Gamir *et al.*, 2012). Maximum g_s and K_{plant} were tightly coordinated in plants growing in the field or in a greenhouse (Fig. 5). Changes in K_{plant}, driven by K_{root}, imposed a decline in g_{s_max}, thus affecting leaf water status and further increases in transpirational water loss and carbon assimilation. Midday Ψ_{leaf} did not change during the flooding treatment, highlighting the adaptive role of stomatal closure in counteracting leaf dehydration (Meinzer, 2003). Furthermore, our data indicate that flooded pines exhibited the same level of reduced K_{plant} as water-stressed plants. Field data showed that red maple exhibited higher hydraulic limitation and higher g_{s_max} in flooded than in water-stressed conditions, indicating that species differences exist in the response to flooding. In contrast, bald cypress and water tupelo regulated the closure of stomata very efficiently, thus adjusting the evaporative water losses to the water uptake capacity of roots and the resulting decrease in K_{plant} (Fig. 5A).

Our results also showed that the sensitivity of g_s to VPD was mostly attributable to the variation in g_{s_max} (Fig. 5B), which is consistent with the isohydric regulation of Ψ_{leaf} induced by K_{plant} (Oren *et al.*, 1999). Stomata responded to VPD in a manner consistent with protecting xylem integrity and thus the capacity for water transport (Domec *et al.*, 2009; McCulloh *et al.*, 2019). Future climate change is expected to increase temperature and therefore VPD in many regions (Oppenheimer *et al.*, 2019). Stomatal acclimation to VPD as affected by drought, flooding, and flooding plus salinity could potentially have a large impact on the global water and carbon cycles. Here we measured that in forested wetlands, global plant transpiration responses to future climate will probably not differ from expectations based on the well-known relationship between g_s and VPD (Oren *et al.*, 1999). To improve climate predictions of warming effects on transpiration for plants subjected to different abiotic stresses, our results indicated that modelers could potentially allow for predictable shifts in g_s under water stress but also flooded conditions, combined with the use of a single coefficient conveying g_s sensitivity to VPD.

Woody species responses to flooding and flooding plus salinity are wide ranging and can change based on the life history stage of a plant. Seedlings are generally more sensitive to salinity, while mature plants may show a wider range of tolerance (Kozlowski, 1997). However, when our field and greenhouse observations were analyzed together, some common responses were observed (Fig. 5), highlighting the need for integrating data on seedlings and mature plants in future studies on wetland adaptation to SLR and its restoration (Carmichael and Smith, 2016).

Conclusion

Our study provides new functional and mechanistic insights on plant hydraulics by showing that the components of K_{plant} are highly dynamic, reflecting a balance between species adaptive capacity and AQP functioning. Neither species tolerated flooding plus salinity. In loblolly pine, high water uptake was largely mediated by active transport through AQP, but was easily disrupted by drought, flooding, and salinity. In bald cypress, a flooding-tolerant species, the contribution of AQP to water transport was less sensitive overall and did not respond to flooding. Under controlled conditions, AQP activity and xylem structure were co-limiting root water transport. However, in response to environmental factors, except again for the flooding treatment in bald cypress, AQP functioning rather than changes in xylem structure or biomass allocation controlled the fluctuations in K_{root}, and thus in K_{plant}. The decline in K_{leaf} was rather the consequence of both a decrease in AQP activity and structural changes. An important challenge was also to integrate the AQP-mediated reduction in K_{root} within the mutual interactions of roots and shoots and its putative effect on gas exchange. As such, across species and treatments, the reduction in g_s and its sensitivity to VPD appeared to be direct responses to decreased K_{plant} and was influenced by the contribution of AQP to water transport.

Supplementary data

The following supplementary data are available at *JXB* online.

Fig. S1. Hydraulic conductance of belowground (root) and aboveground (shoot) components of bald cypress seedlings growing under control conditions.

Fig. S2. Field growth rates in diameter of tree species growing under unflooded or flooded conditions at two sites along the lower coastal plain of eastern North Carolina, USA

Fig. S3. Relationships between whole-plant hydraulic conductance and the percentage of hydraulic resistance in roots, and stomatal conductance and its sensitivity to vapor pressure deficit of species growing under control, water-stressed, flooded, and flooded plus salinity conditions.

Acknowledgements

This work was supported by an USDA-AFRI grant (#2012-00857), the National Science Foundation - Division of Integrative Organismal Systems (#1754893), and by the ANR projects CWSSEA-SEA-Europe and PRIMA-SWATCH (ANR-18-PRIM-0006 and ANR-17-ASIE-0007). The USFWS Alligator River National Wildlife Refuge provided the forested wetland research site, and in-kind support of field operations.

Author contributions

J-CD and DMJ conceived the original screening and research plans; J-CD, DMJ, RW, and MJC performed the hydraulics experiments; ATO, MJC, and RW performed the gas exchange experiments; JSK, J-CD, AN, and GM performed field experiments; WKS provided plant materials; J-CD and DMJ analyzed the data and wrote the article with contributions of all the authors.

Data availability

The data supporting the findings of this study are available from the corresponding author, Jean-Christophe Domec, upon request.

References

Addington RN, Mitchell RJ, Oren R, Donovan LA. 2004. Stomatal sensitivity to vapor pressure deficit and its relationship to hydraulic conductance in *Pinus palustris*. Tree Physiology **24**, 561–569.

Allen JA, Pezeshki SR, Chambers JL. 1996. Interaction of flooding and salinity stress on baldcypress (*Taxodium distichum*). Tree Physiology **16**, 307–313.

Almeida-Rodriguez AM, Hacke UG, Laur J. 2011. Influence of evaporative demand on aquaporin expression and root hydraulics of hybrid poplar. Plant, Cell & Environment **34**, 1318–1331.

Azaizeh H, Steudle E. 1991. Effects of salinity on water transport of excised maize (*Zea mays* L.) roots. Plant Physiology **97**, 1136–1145.

Bhattachan A, Emanuel RE, Ardón M, Bernhardt E, Anderson SM, Stillwagon MG, Ury EA, BenDor TK, Wright JP. 2018. Evaluating the effects of land-use change and future climate change on vulnerability of coastal landscapes to saltwater intrusion. Elementa: Sciences of the Anthropocene **6**, 62.

Boursiac Y, Boudet J, Postaire O, Luu DT, Tournaire-Roux C, Maurel C. 2008. Stimulus-induced downregulation of root water transport involves reactive oxygen species-activated cell signalling and plasma membrane intrinsic protein internalization. The Plant Journal **56**, 207–218.

Bramley H, Turner NC, Turner DW, Tyerman SD. 2009. Roles of morphology, anatomy, and aquaporins in determining contrasting hydraulic behavior of roots. Plant Physiology **150**, 348–364.

Brodersen CR, Germino MJ, Johnson DM, *et al.* 2019. Seedling survival at timberline is critical to conifer mountain forest elevation and extent. Frontiers in Forest and Global Change **2**, 9.

Brodribb TJ, Holbrook NM. 2003. Stomatal closure during leaf dehydration, correlation with other leaf physiological traits. Plant Physiology **132**, 2166–2173.

Carmichael MJ, Smith WK. 2016. Growing season ecophysiology of *Taxodium distichum* (L.) Rich. (bald cypress) saplings in a restored wetland: a baseline for restoration practice. Botany **94**, 1115–1125.

Castonguay Y, Nadeau P, Simard RR. 1993. Effects of flooding on carbohydrate and ABA levels in roots and shoots of alfalfa. Plant, Cell & Environment **16**, 695–702.

Chaumont F, Moshelion M, Daniels MJ. 2005. Regulation of plant aquaporin activity. Biology of the Cell **97**, 749–764.

DeSantis LRG, Bhotika S, Williams K, Putz FE. 2007. Sea-level rise and drought interactions accelerate forest decline on the Gulf Coast of Florida, USA. Global Change Biology **13**, 2349–2360.

Domec JC, King JS, Ward E, *et al.* 2015. Conversion of natural forests to managed forest plantations decreases tree resistance to prolonged droughts. Forest Ecology and Management **355**, 58–71.

Domec JC, Noormets A, King JS, Sun G, McNulty SG, Gavazzi MJ, Boggs JL, Treasure EA. 2009. Decoupling the influence of leaf and root hydraulic conductances on stomatal conductance and its sensitivity to vapour pressure deficit as soil dries in a drained loblolly pine plantation. Plant, Cell & Environment **32**, 980–991.

Domec JC, Palmroth S, Oren R. 2016. Effects of *Pinus taeda* leaf anatomy on vascular and extravascular leaf hydraulic conductance as influenced by N-fertilization and elevated CO_2. Journal of Plant Hydraulics **3**, e007.

Ehlert C, Maurel C, Tardieu F, Simonneau T. 2009. Aquaporin-mediated reduction in maize root hydraulic conductivity impacts cell turgor and leaf elongation even without changing transpiration. Plant Physiology **150**, 1093–1104.

Else MA, Coupland D, Dutton L, Jackson MB. 2001. Decreased root hydraulic conductivity reduces leaf water potential, initiates stomatal closure and slows leaf expansion in flooded plants of castor oil (*Ricinus communis*) despite diminished delivery of ABA from the roots to shoots in xylem sap. Physiologia Plantarum **111**, 46–54.

Farquhar GD, von Caemmerer S, Berry JA. 1980. A biochemical model of photosynthetic CO_2 fixation in leaves of C_3 species. Planta **149**, 78–90.

Gambetta GA, Fei J, Rost TL, Knipfer T, Matthews MA, Shackel KA, Walker MA, McElrone AJ. 2013. Water uptake along the length of grapevine fine roots: developmental anatomy, tissue-specific aquaporin expression, and pathways of water transport. Plant Physiology **163**, 1254–1265.

Gambetta GA, Knipfer T, Fricke W, McElrone AJ. 2017. Aquaporins and root water uptake. In: Chaumont F, Tyerman S eds. Plant aquaporins, signaling and communication in plants. Berlin, Heidelberg: Springer, 133–153.

Hacke UG, Sperry JS, Ewers BE, Ellsworth DS, Schäfer KV, Oren R. 2000. Influence of soil porosity on water use in *Pinus taeda*. Oecologia **124**, 495–505.

Henzler T, Steudle E. 2004. Oxidative gating of water channels (aquaporins) in *Chara* by hydroxyl radicals. Plant, Cell & Environemnt **27**, 1184–1195.

Holbrook NM, Zwieniecki MA. 2003. Plant biology: water gate. Nature **425**, 361.

Johnson DM, Sherrard M, Domec JC, Jackson RB. 2014. Role of aquaporin activity in regulating deep and shallow root hydraulic conductance during extreme drought. Tree Structure and Function **28**, 1223–1331.

Johnson DM, Wortemann R, McCulloh KA, Jordan-Meille L, Ward E, Warren JM, Palmroth S, Domec JC. 2016. A test of the hydraulic

vulnerability segmentation hypothesis in angiosperm and conifer tree species. Tree Physiology **36**, 983–993.

Kamaluddin M, Zwiazek JJ. 2002. Ethylene enhances water transport in hypoxic aspen. Plant Physiology **128**, 962–969.

Keeland BD, Sharitz RR. 1995. Seasonal growth patterns of *Nyssa sylvatica* var. *biflora*, *Nyssa aquatica*, and *Taxodium distichum* as affected by hydrologic regime. Canadian Journal of Forest Research **25**, 1084–1096.

Kirwan ML, Gedan KF. 2019. Sea-level driven land conversion and the formation of ghost forests. Nature Climate Change **9**, 450–457.

Knipfer T, Fricke W. 2011. Water uptake by seminal and adventitious roots in relation to whole-plant water flow in barley (*Hordeum vulgare* L.). Journal of Experimental Botany **62**, 717–733.

Kozlowski TT. 1997. Responses of woody plants to flooding and salinity. Tree Physiology Monograph **1**, 1–29.

Krauss KW, Chambers JL, Allen JA, Luse B, DeBosier A. 1999. Root and shoot responses of *Taxodium distichum* seedlings subjected to saline flooding. Environmental and Experimental Botany **41**, 15–23.

Leyton L, Rousseau Z. 1958. Root growth of tree seedlings in relation to aeration. In: Thimann KV, ed. The physiology of forest trees. New York: Ronald Press, 467–475.

Li X, Wang X, Yang Y, Li R, He Q, Fang X, Luu DT, Maurel C, Lin J. 2011. Single-molecule analysis of PIP2;1 dynamics and partitioning reveals multiple modes of *Arabidopsis* plasma membrane aquaporin regulation. The Plant Cell **23**, 3780–3797.

Loustau D, Crepeau S, Guye MG, Sartore M, Saur E. 1995. Growth and water relations of three geographically separate origins of maritime pine (*Pinus pinaster*) under saline conditions. Tree Physiology **15**, 569–576.

Martinez-Ballesta MC, Martinez V, Carvajal M. 2000. Regulation of water channel activity in whole roots and in protoplasts from roots of melon plants grown under saline conditions. Australian Journal of Plant Physiology **27**, 685–691.

Maurel C, Nacry P. 2020. Root architecture and hydraulics converge for acclimation to changing water availability. Nature Plants **6**, 744–749.

McCulloh KA, Domec JC, Johnson DM, Smith DD, Meinzer FC. 2019. A dynamic yet vulnerable pipeline: integration and coordination of hydraulic traits across whole plants. Plant, Cell & Environment **42**, 2789–2807.

McElrone AJ, Bichler J, Pockman WT, Addington RN, Linder CR, Jackson RB. 2007. Aquaporin-mediated changes in hydraulic conductivity of deep tree roots accessed via caves. Plant, Cell & Environment **30**, 1411–1421.

McLean EH, Ludwig M, Grierson PF. 2011. Root hydraulic conductance and aquaporin abundance respond rapidly to partial root-zone drying events in a riparian *Melaleuca* species. New Phytologist **192**, 664–675.

McLeod KW, McCarron JK, Conner WH. 1996. Effects of flooding and salinity on photosynthesis and water relations of four Southeastern coastal plain forest species. Wetlands Ecology and Management **4**, 31–42.

Megonigal JP, Day FP. 1992. Effects of flooding on root and shoot production of bald cypress in large experimental enclosures. Ecology **73**, 1182–1193.

Meinzer FC. 2003. Functional convergence in plant responses to the environment. Oecologia **134**, 1–11.

Miao G, Noormets A, Domec JC, Trettin CC, McNulty SG, Sun G, King JS. 2013. The effect of water table fluctuation on soil respiration in a lower coastal plain forested wetland in the southeastern US. Journal of Geophysical Research Biogeosciences **118**, 1748–1762.

Munns R. 2002. Comparative physiology of salt and water stress. Plant, Cell & Environment **25**, 239–250.

Munns R, Tester M. 2008. Mechanisms of salinity tolerance. Annual Review of Plant Biology **59**, 651–681.

NAS. 2020. Climate change: evidence and causes: update 2020. Washington, DC: The National Academies Press.

Niinemets U. 2010. Responses of forest trees to single and multiple environmental stresses from seedlings to mature plants: past stress history, stress interactions, tolerance and acclimation. Forest Ecology and Management **260**, 1623–1639.

Oppenheimer M, Glavovic BC, Hinkel J, *et al.* 2019. Sea level rise and implications for low-lying islands, coasts and communities. In: Pörtner HO, Roberts DC, Masson-Delmotte V, ***et al***., eds. IPCC Special Report on the Ocean and Cryosphere in a Changing Climate. IPCC.

Oren R, Sperry JS, Katul GG, Pataki DE, Ewers BE, Phillips N, Schäfer KVR. 1999. Survey and synthesis of intra- and interspecific variation in stomatal sensitivity to vapour pressure deficit. Plant, Cell & Environment **22**, 1515–1526.

Pezeshki SR. 1992. Response of *Pinus taeda* to soil flooding and salinity. Annales des Sciences Forestières **4**, 149–159.

Poulter B, Christensen NL, Song QS. 2008. Tolerance of *Pinus taeda* and *Pinus serotina* to low salinity and flooding: implications for equilibrium vegetation dynamics. Journal of Vegetation Science **19**, 15–22.

Rodríguez-Gamir J, Ancillo G, Legaz F, Primo-Millo E, Forner-Giner MA. 2012. Influence of salinity on PIP gene expression in citrus roots and its relationship with root hydraulic conductance, transpiration and chloride exclusion from leaves. Environmental and Experimental Botany **78**, 163–166.

Rodriguez-Gamir J, Xue J, Clearwater MJ, Meason DF, Clinton PW, Domec JC. 2019. Aquaporin regulation in roots controls plant hydraulic conductance, stomatal conductance, and leaf water potential in *Pinus radiata* under water stress. Plant, Cell & Environment **42**, 717–729.

Siefritz F, Tyree MT, Lovisolo C, Schubert A, Kaldenhoff R. 2002. PIP1 plasma membrane aquaporins in tobacco: from cellular effects to function in plants. The Plant Cell **14**, 869–876.

Sperry JS. 2003. Evolution of water transport and xylem structure. International Journal of Plant Science **164**, 115–127.

Tan X, Zwiazek JJ. 2019. Stable expression of aquaporins and hypoxia-responsive genes in adventitious roots are linked to maintaining hydraulic conductance in tobacco (*Nicotiana tabacum*) exposed to root hypoxia. PLoS One **14**, e0212059.

Titus JG, Richman C. 2001. Maps of lands vulnerable to sea level rise: modeled elevations along the US Atlantic and Gulf coasts. Climate Research **18**, 205–228.

Törnroth-Horsefield S, Wang Y, Hedfalk K, Johanson U, Karlsson M, Tajkhorshid E, Neutze R, Kjellbom P. 2006. Structural mechanism of plant aquaporin gating. Nature **43**, 688–694.

Tyree MT, Sinclair B, Lu P, Granier A. 1993. Whole shoot hydraulic conductance in *Quercus* species measured with a new high-pressure flow meter. Annals of Forest Science **50**, 417–423.

Tyree MT, Zimmermann MH. 2002. Xylem structure and the ascent of sap, 2nd edn. New York: Springer.

Vandeleur RK, Sullivan W, Athman A, Jordans C, Gilliham M, Kaiser BN, Tyerman SD. 2014. Rapid shoot-to-root signalling regulates root hydraulic conductance via aquaporins. Plant, Cell & Environment **37**, 520–538.

Wang N, Palmroth S, Maier CA, Domec JC, Oren R. 2019. Anatomical changes with needle length are correlated with leaf structural and physiological traits across five *Pinus* species. Plant, Cell & Environment **42**, 1690–1704.

Ward EJ, Oren R, Bell DM, Clark JS, McCarthy HR, Kim HS, Domec JC. 2013. The effects of elevated CO_2 and nitrogen fertilization on stomatal conductance estimated from 11 years of scaled sap flux measurements at Duke FACE. Tree Physiology **33**, 135–151.

Woodruff JD, Irish JL, Camargo SJ. 2013. Coastal flooding by tropical cyclones and sea-level rise. Nature **504**, 44–52.

Yang S, Tyree MT. 1994. Hydraulic architecture of *Acer saccharum* and *A. rubrum*: comparison of branches to whole trees and the contribution of leaves to hydraulic resistance. Journal of Experimental Botany **45**, 179–186.

Ye Q, Steudle E. 2006. Oxidative gating of water channels (aquaporins) in corn roots. Plant, Cell & Environment **29**, 459–470.

Zhang J, Zhang X. 1994. Can early wilting of old leaves account for much of the ABA accumulation in flooded leaves? Journal of Experimental Botany **45**, 1335–1342.